Available online at www.sciencedirect.com
ScienceDirect
Journal of Magnetism and Magnetic Materials 308 (2007) 325–340
Journal of magnetism and magnetic materials
www.elsevier.com/locate/jmmm

Review

Review of the magnetocaloric effect in manganite materials

Manh-Huong Phan[a,*], Seong-Cho Yu[b]

[a]Aerospace Composites Group, University of Bristol, Queen's Building, Bristol BS8 1TR, England
[b]Department of Physics, Chungbuk National University, Cheongju 361-763, South Korea

Received 26 June 2006
Available online 17 August 2006

Abstract

A thorough understanding of the magnetocaloric properties of existing magnetic refrigerant materials has been an important issue in magnetic refrigeration technology. This paper reviews a new class of magnetocaloric material, that is, the ferromagnetic perovskite manganites ($R_{1-x}M_xMnO_3$, where R = La, Nd, Pr and M = Ca, Sr, Ba, etc.). The nature of these materials with respect to their magnetocaloric properties has been analyzed and discussed systematically. A comparison of the magnetocaloric effect of the manganites with other materials is given. The potential manganites are nominated for a variety of large- and small-scale magnetic refrigeration applications in the temperature range of 100–375 K. It is believed that the manganite materials with the superior magnetocaloric properties in addition to cheap materials-processing cost will be the option of future magnetic refrigeration technology.

PACS: 75.30.Sg

Keywords: Magnetocaloric effect; Magnetic refrigeration; Magnetic refrigerant materials

1. Introduction

Modern society relies very much on readily available refrigeration. Until now the vapor compression refrigerators have been mainly used for cooling applications. However, the compressing and expanding processes of a gas in these refrigerators are not very efficient because the refrigeration accounts for 25% of residential and 15% of commercial power consumption [1]. In addition, the usage of gases such as chlorofluorocarbons (CFCs) and hydrochlorofluorocarbons (HCFCs) are damaging to our living environment.

Recently, the development of a new magnetic refrigeration (MR) technology, based upon the magnetocaloric effect (MCE) [2], has brought an alternative to the conventional gas compression (CGC) technique [3,4]. The MR technology shows several advantages over the CGC technology [3]. First, the cooling efficiency in magnetic refrigerators is higher (the magnetic cooling efficiency can be reached up to 30–60% of a Carnot cycle, whereas it is only 5–10% for CGC refrigeration) even at a small scale, enabling the development of portable, battery-powered products. Second, magnetic refrigerators can be more compactly built when using solid substances as working materials. Third, the MR does not use ozone-depleting or global-warming gases and therefore is an environmentally friendly cooling technology. It is important to mention that MR has found wide applications in energy-intensive industrial and commercial refrigerators such as large-scale air conditioners, heat pumps, supermarket refrigeration units, waste separation, chemical processing, gas liquification, liquor distilling, sugar refining, grain drying, and so forth [3,4].

MR has long been employed to cooling below 1 K using paramagnetic salts (e.g., $Gd_2(SO_4)_3 \cdot 8H_2O$) [5], but its applications at temperatures around room temperature are not yet commercially available [3], although this technology is believed to be a great new global business [3,4]. Until recently a gadolinium (Gd) rare-earth metal with large MCE has been considered as the most active magnetic refrigerant in room-temperature magnetic refrigerators [3],

*Corresponding author. Tel.: +44 773 766 1390; fax: +44 117 927 2771.
E-mail address: M.H.Phan@bristol.ac.uk (M.-H. Phan).

0304-8853/$ - see front matter © 2006 Elsevier B.V. All rights reserved.
doi:10.1016/j.jmmm.2006.07.025

but its usage is somehow commercially limited because the cost of Gd is quite expensive ~$4000/kg. Therefore, research in the magnetic cooling field has been focused on the search for new materials that are cheaper but displaying larger MCEs [6–10]. As a remarkable breakthrough occurred in 1997, Pecharsky and Gschneidner [6] discovered that the giant magnetocaloric (GMC) effect in a $Gd_5Si_2Ge_2$ alloy was twice larger than in Gd. More importantly, this alloy could not only improve the efficiency of large-scale magnetic refrigerators but also open the door to new small-scale applications, such as home and automotive air conditioning [3]. Nonetheless, the Curie temperature of $Gd_5Si_2Ge_2$ is about 276 K, which is much lower than that of Gd of 294 K, making this alloy difficult to be used in room-temperature magnetic refrigerators [4]. In this context, further efforts to seek for other alternative materials, especially the materials without rare-earth elements, for example, Ni–Mn–Ga alloys [7], Mn–As–Sb alloys [8], La–Fe–Co–S alloys [9], Mn–Fe–P–As alloys [10], La–Ca–Sr–Mn–O manganites [11] and exhibiting large MCEs in the room-temperature range, are also of practical importance.

This review aims to provide a through understanding of the magnetocaloric nature of a new class of manganites and their potentials for active MR (AMR). The advantages and disadvantages of such magnetocaloric manganites are analyzed and discussed, in order to nominate potential magnetocaloric manganites for future MR technology. A comprehensive comparison of the MCE of the manganites with other magnetic refrigerant candidate materials is given. The fundamental aspects of MCE as well as the criteria for selecting magnetic refrigerants for AMR are also discussed.

2. Fundamental aspects

When a magnetic material is subjected to a sufficiently high magnetic field, the magnetic moments of the atoms become reoriented. If the magnetic field is applied adiabatically, the temperature of the material rises, and if the magnetic field is subsequently removed, the temperature decreases. This warming and cooling in response to the application and removal of an external magnetic field is called the 'MCE'. Since the MCE is directly related to the magnetic entropy change and the adiabatic temperature change, it is important to understand the relation between these two quantities.

2.1. Relation between magnetic entropy and adiabatic temperature change

The change of entropy (S) of a magnetic material upon the application of a magnetic field (H) is related to that of magnetization (M) with respect to temperature (T) through the thermodynamic Maxwell relation:

$$\left(\frac{\partial S}{\partial H}\right)_T = -\left(\frac{\partial M}{\partial T}\right)_H. \tag{1}$$

The magnetic entropy change, $\Delta S_M(T,H)$, is calculated by

$$\Delta S_M(T,H) = S_M(T,H) - S_M(T,0) = \int_0^H \left(\frac{\partial M(T,H)}{\partial T}\right)_H \mathrm{d}H. \tag{2}$$

For magnetization measurements made at discrete field and temperature intervals, $\Delta S_M(T,H)$ can be approximately calculated by the following expression:

$$\Delta S_M(T,H) = \sum_i \frac{M_{i+1}(T_{i+1},H) - M_i(T_i,H)}{T_{i+1} - T_i}\,\Delta H. \tag{3}$$

On the other hand, $\Delta S_M(T,H)$ can be obtained from calorimetric measurements of the field dependence of the heat capacity and subsequent integration:

$$\Delta S_M(T,H) = \int_0^T \frac{C(T,H) - C(T,0)}{T}\,\mathrm{d}T, \tag{4}$$

where $C(T,B)$ and $C(T,0)$ are the values of the heat capacity measured in a field H and in zero field ($H = 0$), respectively. Therefore, the adiabatic temperature change (ΔT_{ad}) can be evaluated by integrating Eq. (4) over the magnetic field, which is given by

$$\Delta T_{ad} = -\int_0^H \frac{T}{C_{P,H}}\left(\frac{\partial M}{\partial T}\right)_H \mathrm{d}H. \tag{5}$$

From Eqs. (2) and (5) it is easy to state that a material should have large MCE (i.e., large ΔS_M and ΔT_{ad}) when $(\partial M/\partial T)_H$ is *large* and $C(T,H)$ is *small* at the same temperature [3,4]. Because $(\partial M/\partial T)_H$ peaks the magnetic ordering temperature, a large MCE is often expected close to this magnetic phase transition, and the effect may be further maximized as the change in magnetization with respect to temperature occurs in a narrow temperature interval [4]. It should be noted that although evaluating ΔS_M from magnetization measurements using Eq. (3) has been a useful tool for a rapid screening of potential magnetocaloric materials [3–11], a precise comparison of the MCE among the exiting magnetocaloric materials can only be realized by evaluating ΔT_{ad} instead of ΔS_M [3,4]. This is because the magnitude of heat capacity may be much different from a magnetocaloric material family to another, for example, the heat capacity of a Gd-based alloys system is much smaller than that of a manganite-type materials system [3].

2.2. Relation between magnetic entropy and resistivity

In manganites, both CMR (Colossal magnetoresistive) and MC (magnetocaloric) effects are often observed around the magnetic-ordering phase transition temperature (i.e., the Curie temperature) [11–13] and this evidently suggests that there exists a definite relation between magnetic entropy and resistivity [14–17]. In this case, Xiong et al. [17] proposed a new method that allows evaluating the relation between the magnetic entropy and

resistivity (ρ) of a manganite material by means of

$$\Delta S_M(T,H) = -\alpha \int_0^H \left[\frac{\partial \ln(\rho)}{\partial T}\right]_H \mathrm{d}H \quad (6)$$

with $\alpha = 21.72\,\mathrm{emu/g}$.

It is clear that a larger α leads to a more sensitive dependence of $\Delta S-\rho$. Magnetic disorder, which is characterized by ΔS, affects magnetic polarons that influence the electric transport property thereby leading to the relation of $\Delta S-\rho$ [14,17]. This relation is only valid in a narrow temperature interval, where the magnetic-ordering phase transition occurs [17]. The deviation of Eq. (6) occurring in the low temperature range is because the magnetic polarons are significantly depressed when the system is at a relative magnetic-ordered state [16,17]. In general, the relation (6) provides an alternative method to determine the magnetic entropy change in perovskite manganites from resistive measurements.

2.3. Magnetocaloric behavior and magnetic transition

It is pointed out that the magnitude of the magnetic entropy change and its dependence on temperature and magnetic field are strongly dependent on the nature of the corresponding magnetic phase transition. A first-order field-induced paramagnetic to ferromagnetic transition, which is a magnetic disorder-to-order transition, can give rise to a GMC effect, for example, in Gd–Si–Ge and Mn–Fe–P–As systems [3,4]. However, the field-induced first-order transition, which is a magnetic order-to-order transition, results in a relatively small MCE, for example, in RTiGe and Mn_5Si_3 systems [3].

Most ferromagnetic materials show a second-order magnetic phase transition. It should be noted that a first-order transition is able to concentrate the MCE in a narrow temperature range, whereas second-order transitions are usually spread over a broad temperature range, which is beneficial for AMR [3,4,11]. In addition, there are large thermal and field hystereses for any first-order transitions, which for practical AMR applications should be as small as possible [4].

Furthermore, it is stated that the magnitude of the MCE depends not only on the magnetic moments but also on $\partial M/\partial T$. These larger these values, the higher the MCE. This is the reason why not only rare-earth elements and their compounds have large MCEs [6], but also 3d-based transition–metal compounds can have large MCEs in case of a first-order transition [10]. In the case of manganite materials, it is the rapid change of magnetization with respect to temperature in the magnetic-ordering phase transition range that causes a large magnetic entropy change, i.e., the large MCE [11]. Indeed, Terashita et al. [16] recently revealed that a first-order structural transition in close proximity to the magnetic transition has only little influence on the MCE in doped manganites.

2.4. Magnetic cooling efficiency

The magnetic cooling efficiency of a magnetocaloric material can be, in simple cases, evaluated by considering the magnitude of ΔS_M or ΔT_{ad} and its full-width at half-maximum (δT_{FWHM}) [3,18]. It is easy to establish the product of the ΔS_M maximum and the full-width at half-maximum ($\delta T_{FWHM} = T_2 - T_1$) as

$$\mathrm{RCP}(S) = -\Delta S_M(T,H) \times \delta T_{FWHM}, \quad (7)$$

which stands for the so-called relative cooling power (RCP) based on the magnetic entropy change. An example is displayed in Fig. 1. Similarly, the product of the maximum adiabatic temperature change ΔT_{ad} and the full-width at half-maximum δT_{FWHM} is expressed by

$$\mathrm{RCP}(T) = \Delta T_{ad}(T,H) \times \delta T_{FWHM}, \quad (8)$$

which stands for the so-called RCP based on the adiabatic temperature change.

In short, it is possible to evaluate the magnetic cooling efficiency of a magnetocaloric material by calculating RCP(S) using Eq. (7) or RCP(T) using Eq. (8). In this review, we will evaluate the RCP of magnetocaloric manganites using RCP(S).

2.5. The criteria for selecting magnetic refrigerants

In terms of the theoretical analyses and the magnetocaloric nature of existing materials [3,4], the criteria for selecting magnetic refrigerants for active magnetic refrigerators are given as follows:

- The large magnetic entropy change and the large adiabatic temperature change (i.e., the large MCE).

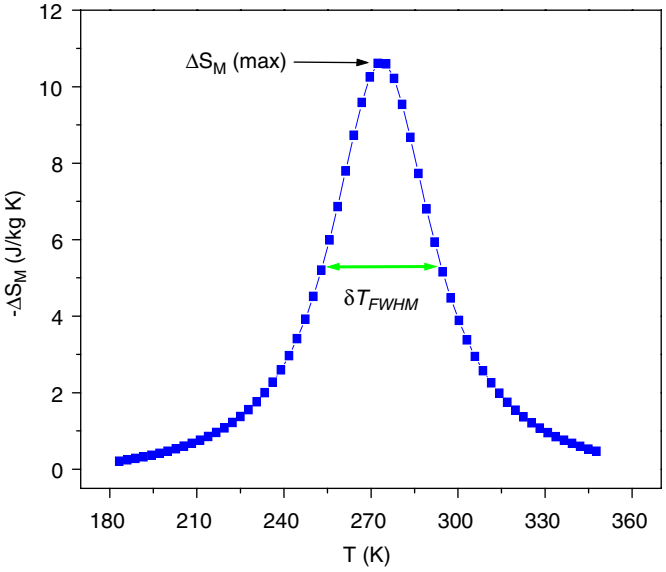

Fig. 1. An example of the evaluation of relative cooling power based on the temperature dependence of magnetic entropy change, RCP(S), for a $La_{0.7}Ca_{0.25}Sr_{0.05}MnO_3$ single crystal.

- The large density of magnetic entropy (it is an important factor contributing to the working efficiency of materials); ferromagnets with large values of effective magnetron number $P = \{J(J+1)\}^{1/2}$ are selected.
- The small lattice entropy (i.e., the high Debye temperature), much attention should be paid to magnetic refrigerants for room-temperature magnetic refrigerators.
- The MCE in the temperature range of 10–80 K or >250 K, where the Curie temperature of a material is located in and, the large magnetic entropy change can be obtained in the whole temperature range of the cycle.
- Nearly zero magnetic hysteresis (it is related to the working efficiency of a magnetic refrigerant material).
- Very small thermal hysteresis (this is related to the reversibility of the MCE of a magnetic refrigerant material).
- Small specific heat and large thermal conductivity (these ensure remarkable temperature change and rapid heat exchange).
- Large electric resistance (i.e., the lowering eddy current heating or the small eddy current loss).
- High chemical stability and simple sample synthesis route are also required for magnetic refrigerant materials.

In addition, for practical AMR applications magnetic refrigerant materials should be less cost.

3. Magnetocaloric measurements

It is possible to measure MCE directly or to calculate MCE indirectly from the measured magnetization or field dependence of the heat capacity, both as a function of temperature and magnetic field [3,4]. It has been shown that, for direct measurement techniques, the accuracy is in the range of 5–10% and depending on the errors in thermometry, errors in field setting, the quality of thermal insulation of the sample, the quality of the compensation scheme to eliminate the effect of the changing magnetic field on the temperature sensor reading [18–21].

For indirect measurement techniques, MCE calculated from magnetization data has quite high errors (~20–30%), whereas MCE calculated from heat capacity data shows a better accuracy than any other techniques at low temperatures. Near room temperature, however, due to the accumulation of experimental errors in the total entropy functions, the errors arising in MCE evaluation become approximately the same as those from direct techniques or indirect magnetization measurements [19,21].

It should be noted that, for first-order phase transition materials, it is not easy to precisely measure MCE. In this case, the MCE calculated from heat capacity should be compared with that measured directly under equilibrium conditions or calculated from magnetization data to ensure that the potentially deleterious effects of intrinsically inaccurate heat capacity have been eliminated or minimized [18,19].

For the case of manganite materials, beside the above-mentioned techniques, MCE can also be evaluated from resistive measurements [17].

4. Manganite materials

In view of the recent literatures, most manganite materials with respect to their magnetocaloric properties have been extensively studied in China, Spain, Brazil, USA, UK, Vietnam and South Korea. In order to clarify whether such manganites can be used as active magnetic refrigerants in magnetic refrigerators, in this section, we will first describe briefly the formation of such a manganite structure that is related directly to its magnetic and magnetocaloric behavior and will then analyze systematically the magnetocaloric properties of this material family. Finally, the MCE features of the manganites are compared with those of other magnetic refrigerant candidate materials.

4.1. Structure

Manganites (or the so-called manganese oxides) have a general formula of $R_{1-x}M_xMnO_3$, where R stands for trivalent rare-earth elements such as La, Pr, Nd, Sm, Eu, Gd, Ho, Tb,Y, etc., and M stands for divalent alkaline earth ions such as Sr, Ca, Ba, and Pb or for Na^{1+}, K^{1+}, Ag^{1+}, etc. The (R,M) site (i.e., the so-called perovskite A-site) can be in most cases formed from homogeneous solid solution [22]. It has been found that these perovskite-based structures occasionally show lattice distortion as modifications from the cubic structure. One of the possible origins in the lattice distortion is the deformation of the MnO_6 octahedron arising from the Jahn–Teller effect that is inherent to the high-spin ($S = 2$) Mn^{3+} with double degeneracy of the e_g orbital. Another lattice deformation comes from the connective pattern of the MnO_6 octahedra in the perovskite structure, forming rhombohedral or orthorhombic lattice. In these distorted perovskites, the MnO_6 octahedra show alternating buckling. Such a lattice distortion of the perovskite in the form of ABO_3 (here $A = R_{1-x}M_x$ and $B = Mn$ for the present manganites) is governed by the so-called tolerance factor t, which is defined as $t = (r_A + r_O)/\sqrt{2}(r_B + r_O)$. Here r_A, r_B and r_O represents the averaged ionic size of each element. The tolerance factor t measures, by definition, the lattice matching of the sequential AO and BO_2 planes. For $t \approx 1$, the cubic perovskite structure is realized. As r_A or t decreases, the lattice structure can be transformed into the rhombohedral ($0.96 < t < 1$) and then into the orthorhombic structure ($t < 0.96$), where the B–O–B bond angle θ is bent and deviated from 180°.

Another important feature in the perovskite and related structures is that the compounds are reasonably appropriate for the carrier-doping procedure (filling control) since this structure is very robust against chemical modifications on the A-site. It important to mention that

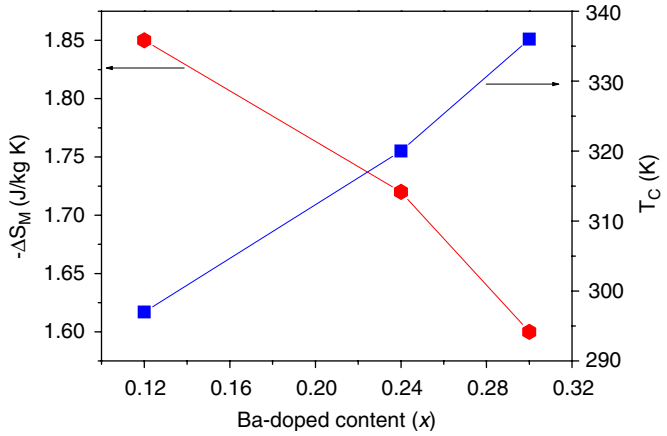

Fig. 2. The dependences of the Curie temperature (T_C) and the magnetic entropy change, ΔS_M, on the Ba-doped concentration (x) for $La_{0.7}Ca_{0.3-x}Ba_xMnO_3$ ($x = 0.12$, 0.24 and 0.3) compounds.

because the magnetic properties of manganites, Curie temperature and saturation magnetization, are strongly doping-dependent, these materials may be good candidates for MR at various temperatures. A representative example of the dependence of the Curie temperature and MCE on doping concentration for $La_{0.7}Ca_{0.3-x}Ba_xMnO_3$ ($x = 0.12$, 0.24, and 0.3) compounds is displayed in Fig. 2.

In general, the conventional solid-state reaction method has been used to synthesize polycrystalline manganite materials. Stoichiometric samples are usually pre-sintered in the temperature range of 700–900 °C for 10–20 h followed by grinding into compound powders. The compound powders are then pressed into pellets and sintered at 900–1300 °C for 15–30 h to give the finished samples. Besides, the sol–gel method has recently been used to synthesize such ceramic materials.

4.2. MCE

For a quick comparison of the MCE of existing manganites, the magnetic entropy change, ΔS_M, the Curie temperature, T_C, the magnetic field change, ΔH, and the relative cooling power, RCP(S), are summarized in Table 1.

4.2.1. $(La_{1-x}M_x)MnO_3$ where $M = Na$, K and Ag

A number of works reported the MCEs in lanthanum manganites with doping M^{1+} ions in the La-site, that is, $La_{1-x}M_xMnO_3$ with M = Na, K and Ag [23–27]. Zhong et al. [23–25] showed that the MCE peak temperature could be tuned in the temperature range of 195–334 K for $La_{1-x}Na_xMnO_3$ compounds and in the temperature range of 230–334 K for $La_{1-x}K_xMnO_3$ compounds. Because these materials also exhibited relatively large MCEs (see Table 1), they could be appropriate for MR in the corresponding temperature ranges.

More interestingly, Tang et al. [26] found the large MCEs in $La_{1-x}Ag_xMnO_3$ ($0 \leqslant x \leqslant 0.3$) manganites. They showed that for $\Delta H = 1$ T, ΔS_M reached a maximum of—3.4 J/kg K for $La_{0.8}Ag_{0.2}MnO_3$; this value is obviously larger than that observed in Gd, $\Delta S_M = -3.1$ J/kg K. By varying Ag concentration of $La_{1-x}Ag_xMnO_3$, Hien et al. [27] revealed that the MCE peak temperature could be tuned in the room-temperature range and the ΔS_M value was the highest for $x = 0.22$ composition (see Table 1). This indicates that $La_{1-x}Ag_xMnO_3$ ($x = 0.2$, 0.22) materials are potential for room-temperature MR. However, the non-uniform distribution of the MCE curve was observed in these samples, which is not desirable for an Ericsson-cycle magnetic refrigerator.

4.2.2. $(La_{1-x}M_x)MnO_3$ where $M = Ca$, Sr, Ba, Cd and Pb

4.2.2.1. $(La_{1-x}Ca_x)MnO_3$. The MCEs of $La_{1-x}M_xMnO_3$ (M = Ca, Sr, Ba) manganite films were first reported by Morelli et al. [28]. However, the obtained ΔS_M values were not very large except that the MCE peak temperature could be tuned in the temperature range of 250–350 K by varying the doping concentration. More interestingly, Guo et al. [29,30] found the large MCEs in $La_{1-x}Ca_xMnO_3$ polycrystalline samples with $0.20 \leqslant x \leqslant 0.33$. It was shown that, for $\Delta H = 1.5$ T, the ΔS_M reached a maximum of about -5.5 J/kg K at 230 K, -4.7 J/kg K at 224 K and -4.3 J/kg K at 260 K for $x = 0.2$, 0.25, and 0.33 compositions, respectively [29]. These values are larger than that of Gd, $\Delta S_M = -4.2$ J/kg K, for the same field change of 1.5 T [3]. In this case, that the large magnetic entropy change produced by the abrupt reduction of magnetization was believed to be attributed to the anomalous thermal expansion just around the Curie temperature [29,30]. Due to this effect, the narrow FWHM of the MCE curve (δT_{FWHM}) for $La_{1-x}Ca_xMnO_3$ ($0.20 \leqslant x \leqslant 0.33$) samples was observed [29]. In contrast, Zhang et al. [31] found a smaller value of ΔS_M of -0.6 J/kg K for $\Delta H = 1$ T and a wider breadth of the MCE peak, $\delta T_{FWHM} = 62$ K, in $La_{0.67}Ca_{0.33}MnO_3$ ($x = 0.33$) than what Guo et al. [29] reported. This discrepancy could arise from the differences in the sample processing routes and/or from the differently chemical composition. In fact, $La_{0.67}Ca_{0.33}MnO_3$ was found to show the largest MCE among the compositions investigated [32–34]. Lin et al. [34] measured the MCE of $La_{0.67}Ca_{0.33}MnO_3$ and found the ΔT_{ad} of 2.4 K for $\Delta H = 2.02$ T. This value of ΔT_{ad} is smaller than that of Gd. It was suggested that the large magnetic entropy change was produced by the abrupt jump in magnetization that is associated with a first-order magnetic phase transition [32,33]. Because of this fact, a drop of the MCE which is related to the change from first- to second-order phase transition was observed [33]. Note that, while the MCE decreased significantly, the MCE cure became more broadening when the material transformed from a first-order phase magnetic transition to a second-order one, which is beneficial for MR [11,33].

The MCEs were also reported in several deficient manganites [35–39]. Xu et al. [35] showed that the $La_{0.54}Ca_{0.32}MnO_{3-\delta}$ deficient manganite had a large ΔS_M of -2.9 J/kg K for $\Delta H = 0.9$ T [35]. Interestingly, the Curie

Table 1
The magnetic ordering temperature and magnetocaloric parameters of the manganite materials in comparison with the two Gd and $Gd_5Si_2Ge_2$ magnetic refrigerant candidate materials

Composition	T_C (K)	ΔH (T)	$-\Delta S_M$ (J/kg K)	RCP(S) (J/kg)	Reference
(La–Na)MnO_3					
$La_{0.925}Na_{0.075}MnO_3$	195	1	1.32	93	[23]
$La_{0.90}Na_{0.10}MnO_3$	218	1	1.53	91	[23]
$La_{0.898}Na_{0.072}Mn_{0.971}O_3$	193	1	1.30	89	[24]
$La_{0.880}Na_{0.999}Mn_{0.977}O_3$	220	1	1.52	87	[24]
$La_{0.835}Na_{0.165}MnO_3$	342	1	2.11	63	[23]
$La_{0.834}Na_{0.163}MnO_{2.99}$	343	1	2.11	63	[24]
$La_{0.80}Na_{0.20}MnO_3$	334	1	1.96	86	[23]
$La_{0.799}Na_{0.199}MnO_{2.97}$	334	1	2.00	90	[24]
(La–K)MnO_3					
$La_{0.893}K_{0.078}Mn_{0.965}O_3$	230	1.5	1.25	195	[25]
$La_{0.877}K_{0.096}Mn_{0.974}O_3$	283	1.5	1.50	180	[25]
$La_{0.813}K_{0.160}Mn_{0.987}O_3$	338	1.5	2.10	128	[25]
$La_{0.796}K_{0.196}Mn_{0.993}O_3$	334	1.5	2.20	119	[25]
(La–Ag)MnO_3					
$La_{0.95}Ag_{0.05}MnO_3$	214	1	1.10	44	[26]
$La_{0.80}Ag_{0.20}MnO_3$	278	1	3.40	41	[26]
$La_{0.80}Ag_{0.20}MnO_3$	300	1	2.40	32	[27]
$La_{0.78}Ag_{0.22}MnO_3$	306	1	2.90	38	[27]
$La_{0.75}Ag_{0.25}MnO_3$	306	1	1.52	45	[26]
$La_{0.70}Ag_{0.30}MnO_3$	306	1	1.35	33	[26]
(La–Ca)MnO_3					
$La_{0.80}Ca_{0.20}MnO_3$	230	1.5	5.50	72	[29]
$La_{0.80}Ca_{0.20}MnO_3$	176	1.5	3.67	110	[81]
$La_{0.75}Ca_{0.25}MnO_3$	224	1.5	4.70	99	[30]
$La_{0.70}Ca_{0.30}MnO_3$	256	1	1.38	41	[80]
$La_{0.70}Ca_{0.30}MnO_3$	227	1	1.95	49	[79]
$La_{0.54}Ca_{0.32}MnO_{3-\delta}$	272	0.9	2.90	31	[35]
$La_{0.67}Ca_{0.33}MnO_3$	260	1.5	4.30	47	[29]
$La_{0.67}Ca_{0.33}MnO_3$	259	3	2.60	114	[31]
$La_{0.67}Ca_{0.33}MnO_3$	252	5	2.06	175	[28]
$La_{0.67}Ca_{0.33}MnO_{3-\delta}$	260	1	5.00	35	[36]
$La_{2/3}Ca_{1/3}MnO_3$	267	3	6.40	134	[32]
$La_{0.60}Ca_{0.40}MnO_3$	263	3	5.00	135	[83]
$La_{0.55}Ca_{0.45}MnO_3$	238	1.5	1.90	68	[29]
(La–Sr)MnO_3					
$La_{0.87}Sr_{0.13}MnO_3$	197	5	5.80	232	[12]
$La_{0.845}Sr_{0.155}MnO_3$	234	7	6.60	396	[20]
$La_{0.845}Sr_{0.155}MnO_3$	310	1.35	1.72	61	[54]
$La_{0.84}Sr_{0.16}MnO_3$	244	5	5.85	240	[12]
$La_{0.88}Sr_{0.120}MnO_3$	152	7	6.00	372	[21]
$La_{0.865}Sr_{0.135}MnO_3$	200	7	4.40	330	[21]
$La_{0.845}Sr_{0.155}MnO_3$	235	7	6.7	670	[21]
$La_{0.815}Sr_{0.185}MnO_3$	280	7	7.1	533	[21]
$La_{0.800}Sr_{0.200}MnO_3$	305	7	7.9	395	[21]
$La_{0.75}Sr_{0.25}MnO_3$	340	1.5	1.50	65	[47]
$La_{0.65}Sr_{0.35}MnO_3$	305	1	2.12	106	[13]
$La_{0.67}Sr_{0.33}MnO_3$	348	5	1.69	211	[28]
$La_{2/3}Sr_{1/3}MnO_3$	370	1	1.50	41	[33]
(La–Ba)MnO_3					
$La_{0.7}Ba_{0.3}MnO_3$	336	1	1.60	36	[42]
$La_{0.67}Ba_{0.33}MnO_3$	292	5	1.48	161	[28]
$La_{2/3}Ba_{1/3}MnO_3$	337	1	2.70	68	[43]
$La_{2/3}Ba_{1/3}MnO_{2.98}$	312	1	2.60	65	[43]
$La_{2/3}Ba_{1/3}MnO_{2.95}$	300	1	2.55	69	[43]
$La_{2/3}Ba_{1/3}MnO_{2.92}$	275	1	1.80	90	[43]
$La_{2/3}Ba_{1/3}MnO_{2.9}$	268	1	1.70	94	[43]
(La–Cd)MnO_3					
$La_{0.8}Cd_{0.2}MnO_3$	155	1.35	1.01	32	[44]

Table 1 (*continued*)

Composition	T_C (K)	ΔH (T)	$-\Delta S_M$ (J/kg K)	RCP(S) (J/kg)	Reference
$La_{0.7}Cda_{0.3}MnO_3$	150	1.35	2.88	86	[44]
(La–Pb)MnO$_3$					
$La_{0.9}Pb_{0.1}MnO_3$	235	1.35	0.65	—	[45]
$La_{0.8}Pb_{0.2}MnO_3$	310	1.35	1.30	—	[45]
$La_{0.7}Pb_{0.3}MnO_3$	358	1.35	1.53	53	[45]
$La_{0.6}Pb_{0.4}MnO_3$	360	1.35	0.87	—	[45]
$La_{0.5}Pb_{0.5}MnO_3$	355	1.35	0.81	31	[45]
$La_{0.9}Pb_{0.1}MnO_3$	160	1.5	0.53	—	[46]
$La_{0.8}Pb_{0.2}MnO_3$	294	1.5	1.22	92	[46]
$La_{0.7}Pb_{0.3}MnO_3$	352	1.5	0.96	48	[46]
(La–Ca–Sr)MnO$_3$					
$La_{0.75}Ca_{0.125}Sr_{0.125}MnO_3$	282	1.5	1.50	108	[47]
$La_{0.75}Ca_{0.1}Sr_{0.15}MnO_3$	325	1.5	2.85	72	[47]
$La_{0.75}Ca_{0.075}Sr_{0.175}MnO_3$	330	1.5	2.80	70	[47]
$La_{2/3}(Ca_{0.95}Sr_{0.05})_{1/3}MnO_3$	275	1	3.26	71	[33]
$La_{2/3}(Ca_{0.85}Sr_{0.15})_{1/3}MnO_3$	287	1	2.15	52	[33]
$La_{2/3}(Ca_{0.75}Sr_{0.25})_{1/3}MnO_3$	300	1	1.80	54	[33]
$La_{2/3}(Ca_{0.50}Sr_{0.50})_{1/3}MnO_3$	337	1	1.70	38	[33]
$La_{2/3}(Ca_{0.25}Sr_{0.75})_{1/3}MnO_3$	366	1	1.65	37	[33]
$La_{0.7}Ca_{0.25}Sr_{0.05}MnO_3$	275	5	10.5	462	[11]
$La_{0.7}Ca_{0.20}Sr_{0.10}MnO_3$	308	5	7.45	374	[11]
$La_{0.7}Ca_{0.10}Sr_{0.20}MnO_3$	340	5	6.97	369	[11]
$La_{0.7}Ca_{0.05}Sr_{0.25}MnO_3$	341	5	6.86	364	[11]
$La_{0.6}Ca_{0.2}Sr_{0.2}MnO_3$	337	1	1.96	117	[13]
(La–Ca–Ba)MnO$_3$					
$La_{0.7}Ca_{0.18}Ba_{0.12}MnO_3$	298	1	1.85	45	[42]
$La_{0.7}Ca_{0.06}Ba_{0.24}MnO_3$	320	1	1.72	44	[42]
(La–Ca–Pb)MnO$_3$					
$La_{2/3}(Ca,Pb)_{1/3}MnO_3$	290	7	7.5	375	[14]
$La_{0.6}Ca_{0.3}Pb_{0.1}MnO_3$	289	1.35	2.55	56	[53]
$La_{0.7}Ca_{0.2}Pb_{0.1}MnO_3$	295	1.35	2.53	45	[53]
$La_{0.7}Ca_{0.1}Pb_{0.2}MnO_3$	337	1.35	3.72	71	[53]
(La–Y–Ca)MnO$_3$					
$La_{0.60}Y_{0.07}Ca_{0.33}MnO_3$	230	3	1.46	140	[32]
(La–Bi–Ca)MnO$_3$					
$La_{0.62}Bi_{0.05}Ca_{0.33}MnO_3$	248	1	3.50	53	[56]
$La_{0.62}Bi_{0.05}Ca_{0.33}MnO_3$	248	2	5.30	125	[56]
(La–Nd–Ca)MnO$_3$					
$La_{0.65}Nd_{0.05}Ca_{0.30}MnO_3$	247	1	1.68	47	[55]
$La_{0.60}Nd_{0.10}Ca_{0.30}MnO_3$	233	1	1.95	37	[55]
$La_{0.55}Nd_{0.15}Ca_{0.30}MnO_3$	224	1	2.15	56	[55]
$La_{0.50}Nd_{0.20}Ca_{0.30}MnO_3$	213	1	2.31	60	[55]
(La–Nd–Ba)MnO$_3$					
$La_{0.65}Nd_{0.05}Ba_{0.3}MnO_3$	325	1	1.57	24	[52]
$La_{0.63}Nd_{0.07}Ba_{0.3}MnO_3$	307	1	1.59	26	[52]
$La_{0.6}Nd_{0.1}Ba_{0.3}MnO_3$	285	1	1.85	27	[52]
$La_{0.55}Nd_{0.15}Ba_{0.3}MnO_3$	269	1	2.22	31	[52]
(La–R–Ca)MnO$_3$					
$(La_{0.9}Tb_{0.1})_{2/3}Ca_{1/3}MnO_3$	166	1.5	4.76	95	[57]
$(La_{0.9}Dy_{0.1})_{2/3}Ca_{1/3}MnO_3$	176	1.5	6.06	108	[57]
$(La_{0.9}Gd_{0.1})_{2/3}Ca_{1/3}MnO_3$	182	1.5	5.78	124	[57]
$(La_{0.9}Ce_{0.1})_{2/3}Ca_{1/3}MnO_3$	244	1.5	4.53	72	[57]
(La–Sr–Ba)MnO$_3$					
$La_{0.6}Sr_{0.2}Ba_{0.2}MnO_3$	354	1	2.26	67	[13]
(La–Ca)(Ti–Mn)O$_3$					
$La_{0.65}Ca_{0.35}Ti_{0.4}Mn_{0.6}O_3$	42	3	0.6	55	[59]
$La_{0.65}Ca_{0.35}Ti_{0.2}Mn_{0.8}O_3$	87	3	0.9	123	[59]
$La_{0.65}Ca_{0.35}Ti_{0.1}Mn_{0.9}O_3$	103	3	1.3	182	[59]

Table 1 (*continued*)

Composition	T_C (K)	ΔH (T)	$-\Delta S_M$ (J/kg K)	RCP(S) (J/kg)	Reference
(La–Li)(Ti–Mn)O_3					
$La_{0.83}Li_{0.17}Ti_{0.4}Mn_{0.6}O_3$	35	3	0.9	65	[59]
$La_{0.85}Li_{0.15}Ti_{0.3}Mn_{0.7}O_3$	60	3	1.1	89	[59]
$La_{0.917}Li_{0.05}Ti_{0.2}Mn_{0.8}O_3$	77	3	1.7	121	[59]
$La_{0.958}Li_{0.025}Ti_{0.1}Mn_{0.9}O_3$	90	3	2.0	128	[59]
(La–Sr)(Mn–Ni)O_3					
$La_{0.7}Sr_{0.3}Mn_{0.99}Ni_{0.01}O_3$	—	1.35	2.67	—	[64]
$La_{0.7}Sr_{0.3}Mn_{0.98}Ni_{0.02}O_3$	325	1.35	3.54	71	[64]
$La_{0.7}Sr_{0.3}Mn_{0.97}Ni_{0.03}O_3$	—	1.35	3.15	—	[64]
$La_{0.7}Sr_{0.3}Mn_{0.95}Ni_{0.05}O_3$	—	1.35	2.33	—	[64]
$La_{0.7}Sr_{0.3}Mn_{0.98}Ni_{0.02}O_3$	350	7	7.65	459	[65]
(La–Sr)(Mn–Cu)O_3					
$La_{0.845}Sr_{0.155}Mn_{0.9}Cu_{0.1}O_3$	265	1.35	2.76	61	[54]
$La_{0.7}Sr_{0.3}Mn_{0.95}Cu_{0.05}O_3$	350	1.35	1.96	39	[62]
$La_{0.7}Sr_{0.3}Mn_{0.90}Cu_{0.10}O_3$	350	1.35	2.07	43	[62]
$La_{0.7}Sr_{0.3}Mn_{0.95}Cu_{0.05}O_3$	346	1.5	5.20	312	[63]
$La_{0.7}Sr_{0.3}Mn_{0.90}Cu_{0.10}O_3$	348	1.5	5.51	330	[63]
(La–Sr)(Mn–M)O_3					
$La_{0.67}Sr_{0.33}Mn_{0.9}Cr_{0.1}O_3$	328	5	5.00	200	[61]
$La_{0.845}Sr_{0.155}Mn_{0.98}Co_{0.02}O_3$	230	1.35	2.25	52	[54]
(La–Nd–Ca)(Mn–M)O_3					
$La_{0.65}Nd_{0.05}Ca_{0.3}MnO_3$	250	1	1.68	40	[66]
$La_{0.65}Nd_{0.05}Ca_{0.3}Mn_{0.9}Cr_{0.1}O_3$	225	1	0.96	98	[66]
$La_{0.65}Nd_{0.05}Ca_{0.3}Mn_{0.9}Fe_{0.1}O_3$	150	1	0.42	37	[66]
(Nd–Sr)(Mn–M)O_3					
$Nd_{0.5}Sr_{0.5}MnO_3$	155[a]	1	2.8	17	[67]
$Nd_{0.5}Sr_{0.5}MnO_3$	155[a]	1.35	1.9	15	[69]
$Nd_{0.5}Sr_{0.5}Mn_{0.98}Cu_{0.02}O_3$	170[a]	1.35	0.9	—	[69]
$Nd_{0.5}Sr_{0.5}Mn_{0.90}Cu_{0.10}O_3$	260	1.35	1.25	—	[69]
(Pr–Ca)MnO_3					
$Pr_{0.68}Ca_{0.32}MnO_3$	21.5	5	24	—	[70]
$Pr_{0.68}Ca_{0.32}MnO_3$	31	5	27	—	[70]
(Pr–Sr)MnO_3					
$Pr_{0.5}Sr_{0.5}MnO_3$	160[a]	1	7.10	—	[73]
$Pr_{0.63}Sr_{0.37}MnO_3$	300	5	8.52	511	[74]
(Pr–Pb)MnO_3					
$Pr_{0.9}Pb_{0.1}MnO_3$	150	1.35	3.91	38	[75]
$Pr_{0.8}Pb_{0.2}MnO_3$	175	1.35	2.64	55	[75]
$Pr_{0.7}Pb_{0.3}MnO_3$	225	1.35	2.81	57	[75]
$Pr_{0.6}Pb_{0.4}MnO_3$	254	1.35	3.68	33	[75]
$Pr_{0.5}Pb_{0.5}MnO_3$	253	1.35	3.34	31	[75]
(Nd–Pr–Sr)MnO_3					
$Nd_{0.25}Pr_{0.25}Sr_{0.5}MnO_3$	170	1.35	1.65	24	[69]
(La–Ca)Mn_2O_7					
$La_{1.6}Ca_{1.4}Mn_2O_7$	168	1.5	3.8	160	[76]
$La_{1.4}Ca_{1.6}Mn_2O_7$	270	5	16.8	420	[77]
Gd	294	5	10.2	410	[3]
$Gd_5Si_2Ge_2$	276	5	18.4	535	[3]

[a]The charge-order transition temperature, T_{co}.

temperature of this sample is ~272 K, about 10 K higher than that of the $La_{0.67}Ca_{0.33}MnO_3$ compound. This indicates that $La_{0.54}Ca_{0.32}MnO_{3-\delta}$ could be used as active magnetic refrigerants in sub-room-temperature magnetic refrigerators. In another investigation, Hueso et al. [36] revealed the possibility of tuning the MCE peak temperature without suppressing large MCE values of $La_{0.67}Ca_{0.33}MnO_{3-\delta}$ nanoparticles synthesized by sol–gel techniques. It should be, however, noted that the magnitude of ΔS_M was found to be inversely proportional to the grain size [36]. Phan et al. [37,38] also investigated the magnetic and magnetocaloric properties of $(La_{1-x})_{0.8}$-

$Ca_{0.2}MnO_3$ ($x = 0.05$, 0.10, 0.20, and 0.30) with deficient La-site vacancies. It is interesting that the increase in La-deficiency favored not only the MCE but also lifted the Curie temperature up to higher values, which is beneficial for MR at various temperatures. Recently, Hou et al. [39] also investigated the MCEs of $La_{0.67-x}Ca_{0.33}MnO_3$ ($x = 0$, 0.02, 0.06, and 0.1) deficient samples. The largest ΔS_M value was obtained to be -2.78 J/kg K at 277 K for $\Delta H = 1$ T for the $x = 0.02$ sample. This material could be good for sub-room-temperature MR.

4.2.2.2. $(La_{1-x}Sr_x)MnO_3$. In order to tailor MCEs in the room-temperature range, several efforts were made to explore the MCEs of $La_{1-x}Sr_xMnO_3$ manganites [12,20,21,33,40,41]. Szewczyk et al. [20] first reported the MCE of a $La_{0.845}Sr_{0.155}MnO_3$ polycrystalline manganite, which underwent a magnetic phase transition at 234 K. The ΔS_M and ΔT_{ad} reached, respectively, -6.6 J/kg K and 3.3 K for $\Delta H = 7$ T. Later on, these authors [21] measured systematically the MCEs of $La_{1-x}Sr_xMnO_3$ ($x = 0.120$, 0.135, 0.155, 0.185, and 0.200) manganites. It was shown that the MCE increased with increasing Sr-doped content, expect for $x = 0.120$ composition. The ΔT_{ad} reached the highest value of 4.15 K for $\Delta H = 7$ T for $x = 0.200$ composition [21]. In an analogous manner, Demin and Koroleva [40] also found that the MCE increased in $La_{1-x}Sr_xMnO_3$ ($0.1 < x < 0.3$) single crystals with Sr addition. For $\Delta H = 0.82$ T, the obtained ΔT_{ad} values were 0.2 K at 175 K for $x = 0.1$, 0.37 K at 180 K for $x = 0.125$, 0.7 at 160 K for $x = 0.175$, and 0.78 K at 346 K for $x = 0.3$. Mira et al. [33] found the ΔS_M of -1.5 J/kg K at 370 K for $\Delta H = 1$ T in the $La_{0.67}Sr_{0.33}MnO_3$ polycrystalline sample. This result is quite similar to that of Xu et al. [41]. Most interestingly, the large ΔS_M value of -2.12 J/kg K at 305 K for $\Delta H = 1$ T was reported by Phan et al. [13] in $La_{0.65}Sr_{0.35}MnO_3$. This material is potential for room-temperature MR.

4.2.2.3. $(La_{1-x}Ba_x)MnO_3$. The MCE of a $La_{0.7}Ba_{0.3}MnO_3$ polycrystalline manganite was first measured by Phan et al. [42]. They found the ΔS_M of -1.6 J/kg K at 336 K for $\Delta H = 1$ T. Zhong et al. [43] studied the effects of oxygen stoichiometry on the magnetic and magnetocaloric properties of $La_{2/3}Ba_{1/3}MnO_{3-\delta}$ ($\delta = 0$, 0.02, 0.05, 0.08, and 0.1) samples. They observed a considerable reduction of the MCE in the samples with oxygen deficiency. It is interesting to note that the $La_{2/3}Ba_{1/3}MnO_{3-\delta}$ ($\delta = 0.0$) sample exhibited a large ΔS_M of -2.7 J/kg K at 350 K for $\Delta H = 1$ T [43]. This result is quite different from that reported by Xu et al. [41] on the $La_{0.67}Ba_{0.33}MnO_3$ composition. This discrepancy could be caused by the differences in the sample preparation and the chemical composition [41,43]. In general, the $La_{2/3}Ba_{1/3}MnO_3$ material is suitable for room-temperature MR.

4.2.2.4. $(La_{1-x}Cd_x)MnO_3$. Luong et al. [44] investigated the MCEs of $La_{1-x}Cd_xMnO_3$ ($x = 0.1$, 0.2, and 0.3) manganites. It was shown that, for $\Delta H = 1.35$ T, ΔS_M reached -2.88 J/kg K at 140 K for $x = 0.3$ and -1.01 J/kg K at 150 K for $x = 0.2$. No MCE was reported for $x = 0.1$ composition. It was noted that the temperature at which the ΔS_M peaked did not coincide with the magnetic-ordering phase transition temperature (T_C), unlike other magnetocaloric manganites [11,13]. In addition, the resistivity of the sample increased with increasing Cd concentration. These anomalous features could be attributed to the non-uniform distribution of grains in these samples.

4.2.2.5. $(La_{1-x}Pb_x)MnO_3$. Chau et al. [45] investigated systematically the electrical, magnetic and magnetocaloric properties of $La_{1-x}Pb_xMnO_3$ ($x = 0.1$, 0.2, 0.3, 0.4, and 0.5) manganites. They found that the ΔS_M increased with increasing Pb-doped concentration up to $x = 0.3$ and then decreased for higher Pb-doping level. The largest ΔS_M was -1.53 J/kg K at 358 K for $\Delta H = 1.35$ T for $La_{0.7}Pb_{0.3}MnO_3$ ($x = 0.3$) sample. In turn, Min et al. [46] measured both ΔS_M and ΔT_{ad} of $La_{1-x}Pb_xMnO_3$ ($x = 0.1$, 0.2 and 0.3) samples and showed that, among the compositions investigated, the largest ΔS_M value was obtained for $x = 0.2$ composition. However, for $\Delta H = 1.5$ T, the ΔT_{ad} was obtained to be about 0.68 and 1 K for $x = 0.2$ and 0.3 at 292 and 349 K, respectively. In this case, the authors [46] stated that, because the heat capacity of Pb is larger compared to La, the ΔT_{ad} was larger for the $x = 0.3$ sample than for the $x = 0.2$ sample. It is clear that, though the ΔS_M and ΔT_{ad} could be obtained in the room-temperature range, these values were quite small and therefore not desirable for room-temperature AMR.

4.2.3. (La–Ca–M)MnO_3 where M = Sr, Ba, and Pb

$La_{1-x}Ca_xMnO_3$ phases exhibited the largest MCEs among the existing manganites, but their Curie temperatures are quite below room temperature, for example, the maximum $T_C = 267$ K for $La_{0.67}Ca_{0.33}MnO_3$ [29–34]. This probably limits the usage of $La_{1-x}Ca_xMnO_3$ materials for AMR in the room-temperature range. In this context, such substitution of Ca by other elements with larger ionic radius such as Sr, Ba, and Pb could be of significant importance, because this could allow increasing T_C while still retaining relatively large MCE values.

Indeed, it was shown that the substitution of Sr small amount for Ca in $La_{1-x}Ca_xMnO_3$ could tune the MCE peak temperature in the temperature range of 150–300 K, while retaining relatively large MCE values [11,13,33,47–51]. Most interestingly, Phan et al. [11,51] reported the room-temperature large MCEs of $La_{0.7}Ca_{0.3-x}Sr_xMnO_3$ ($x = 0.05$, 0.10, 0.20, and 0.25) single crystals. For $\Delta H = 5$ T, the ΔS_M reached a maximum value of -10.5 J/kg K at 275 K for $x = 0.05$ composition, which is larger than that of Gd, $\Delta S_M = -10.2$ J/kg K at 294 K. In addition, the large values of ΔS_M were obtained for the remaining samples in the room-temperature range (see Table 1). Therefore, these single crystals are attractive candidate materials for room-temperature AMR. For the

case of $La_{2/3}(Ca_{1-x}Sr_x)_{1/3}MnO_3$ ($x = 0$, 0.05, 0.15, 0.25, 0.50, 0.75, and 1) polycrystalline samples, the drop of the MCE value was observed as the Sr-substituted content increased [33]. For $\Delta H = 1\,T$, the ΔS_M decreased from $-3.7\,J/kg\,K$ for $La_{2/3}Ca_{1/3}MnO_3$ to $-1.5\,J/kg\,K$ for $La_{2/3}Sr_{1/3}MnO_3$. This is probably because the system changed from orthorhombic (Pbnm) to rhomboheral (R3c) structure accompanying by the respective magnetic phase transition from first- to second-order [33]. To this extent, Guo et al. [47] also proposed that, in a fixed crystal structure with orthorhombic or rhombohedral phase, the magnetic entropy change decreased with increasing the A-site ionic average radius, $\langle r_A \rangle$.

When substituting Ba partially for Ca, Phan et al. [42] found the large magnetic entropy changes above 300 K in $La_{0.7}Ca_{0.3-x}Ba_xMnO_3$ ($x = 0.12$, 0.24, and 0.3) compounds. It was found that the ΔS_M decreased with increasing Ba-doping level. For $\Delta H = 1\,T$, the ΔS_M was $-1.85\,J/kg\,K$ at 298 K for $x = 0.12$, $-1.72\,J/kg\,K$ at 320 K for $x = 0.24$, and $-1.6\,J/kg\,K$ at 336 K for $x = 0.3$. These materials are suitable for room-temperature MR. Further investigation into this work [42], Chen et al. [52] substituted Nd for La in $La_{0.7-x}Nd_xBa_{0.3}MnO_3$ ($x = 0$, 0.05, 0.07, 0.1 and 0.15) samples. It was shown that, with increasing Nd-doping level, the ΔS_M significantly increased, while the Curie temperature gradually decreased (see Table 1). Because the Curie temperatures range from 269 to 333 K, these materials could be used as magnetic refrigerants for MR in the sub-room and room-temperature range.

Sun et al. [14] investigated the MCE of $La_{2/3}(Ca,Pb)_{1/3}MnO_3$, which underwent a transition from paramagnetic insulator to ferromagnetic metal temperature around 290 K. They found the $\Delta S_M = -7.5\,J/kg\,K$ and the $\Delta T_{ad} = 5.6\,K$ for $\Delta H = 7\,T$. This ΔS_M value is smaller than that of $La_{2/3}Ca_{1/3}MnO_3$, for the same magnetic field change [3,14]. More interestingly, Phan et al. [53] investigated the MCEs of $La_{0.6}Ca_{0.3}Pb_{0.1}MnO_3$, $La_{0.7}Ca_{0.2}Pb_{0.1}MnO_3$, and $La_{0.7}Ca_{0.1}Pb_{0.2}MnO_3$ samples and found the largest ΔS_M of $-3.72\,J/kg\,K$ at 337 K for $\Delta H = 1.35\,T$ for the third sample. The large ΔS_M of $-2.26\,J/kg\,K$ at 354 K for $\Delta H = 1\,T$ was also observed for $La_{0.6}Sr_{0.2}Ba_{0.2}MnO_3$ [13]. Such materials are promising for room-temperature AMR.

It is stated that any substitution of M (= Sr, Ba and Pb) for Ca in (La–Ca–M)MnO_3 manganites usually leads to an increase in T_C but to a reduction in the MCE. However, a proper combination of both the MCE and the Curie temperature can produce appropriate magnetic refrigerants for room-temperature magnetic refrigerators. Furthermore, the increase in the average A-site ionic radius could be attributed to the increase of the T_C, while the slight decrease in the maximum ΔS_M probably originates from the decrease of spin–lattice interaction. Following this hypothesis, Phan et al. [54] used successfully the electron paramagnetic resonance (EPR) method to study the effects of the spin–lattice coupling on changes of the magnetic entropy in the magnetic-ordering phase transition range in doped manganites.

4.2.4. (La–M–Ca)MnO_3 where M = Nd, Cd, Bi, Tb, Dy, Gd and Ce

It was shown that MCE could be improved in (La–M–Ca)MnO_3 manganites with La substituted by other elements such as M = Nd, Bi, Tb, Gd, and Ce. Wang et al. [55] investigated the MCEs of $La_{0.7-x}Nd_xCa_{0.3}MnO_3$ ($x = 0$, 0.05, 0.1, 0,15, and 0.2) compounds with Nd substitution for La. The largest ΔS_M value was obtained to be $-2.31\,J/kg\,K$ at 213 K for $\Delta H = 1\,T$ for $x = 0.2$ composition. The Nd addition in the precursor $La_{0.7}Ca_{0.3}MnO_3$ sample shifted the MCE peak towards lower temperatures, which are well below room temperature. This perhaps limits the usage of $La_{0.7-x}Nd_xCa_{0.3}MnO_3$ materials for the purpose of room-temperature MR. However, these materials are good for MR in the temperature range of 210–270 K.

In an analogous manner, the substitution of Bi (5 at%) for La in $La_{0.67}Ca_{0.33}MnO_3$ was found to significantly improve the MCE [56]. For $\Delta H = 1\,T$, the $La_{0.62}Bi_{0.05}Ca_{0.33}MnO_3$ ($x = 0.05$) sample exhibited a large ΔS_M of $-3.5\,J/kg\,K$ at 248 K. This value of ΔS_M is slightly larger than that of the precursor sample of $La_{0.67}Ca_{0.33}MnO_3$ ($x = 0$). In this case, it should be noted that though the MCE was enhanced, the remarkable drop of T_C could make it difficult to be used in room-temperature magnetic refrigerators. In another work, Zhang et al. [32] revealed that the partial substitution of La by Y in the $La_{0.67-x}Y_xCa_{0.33}MnO_3$ ($x = 0.07$) sample resulted in a decrease of both the MCE and T_C.

Another study of the magnetocaloric properties of $(La_{1-x}M_x)_{2/3}Ca_{1/3}MnO_3$ (M = Gd, Dy, Tb, Ce) compounds was made by Chen et al. [57]. It was shown that partial substitution of La by rare-earth elements caused a decrease in T_C, and the highest ΔS_M value was obtained for all $x = 0.1$ rare-earth dopants (see Table 1). The $(La_{1-x}R_x)_{2/3}Ca_{1/3}MnO_3$ materials are suitable for MR in the temperature range of 80–260 K. More interestingly, Wang et al. [58] recently reported a large MCE with broadened FWHM in $(La_{0.47}Gd_{0.2})Sr_{0.33}MnO_3$ polycrystalline nanoparticles. This material could be appropriate for sub-room AMR.

4.2.5. (La–M)(Mn–M′)O_3 where M = Ca, Li, Sr and M′ = Ti, Cr, Cu, Co, Ni

Since the magnetic property is also governed by the strength of double-exchange interaction of Mn^{3+}–O–Mn^{4+}, doping at the Mn-site could be of interest in modifying the double-exchange strength and hence the magnetic and magnetocaloric behavior of a doped manganite.

Bohigas et al. [59] first showed that, when substituting Ti partially for Mn in $La_{0.65}Ca_{0.35}Ti_{1-x}Mn_xO_3$ and $La_{0.5+x+y}Li_{0.5-3y}Ti_{1-3x}Mn_{3x}O_{3-z}$ systems, the MCE peak temperature could be tuned in the wide temperature

range of 35–263 K and this is desirable for the active magnetic refrigerator materials suggested by Barclay [60].

Sun et al. [61] found a decrease of both MCE and T_C in $La_{0.67}Sr_{0.33}Mn_{1-x}Cr_xO_3$ ($x = 0$, 0.1) manganites with Cr partial substitution for Mn. For $\Delta H = 6$ T, $La_{0.67}Sr_{0.33}Mn_{0.9}Cr_{0.1}O_3$ has the maximum ΔS_M of -5.8 J/kg K at ~337 K. Nonetheless, this value is quite large and is therefore suitable for MR above room temperature. Furthermore, it was noted that a shoulder peak observed at ~337 K developed under high magnetic fields. Consequently, the magnetic entropy peak was broadened, which is beneficial for an Ericsson-cycle MR. The shoulder peak could imply that the microscopic magnetic structure above T_C was not simple paramagnetic state due to the complex magnetic interactions induced by Cr doping [61].

Recently, Chau et al. [62] investigated the influence of Cu partial substitution for Mn on the MCE of $La_{0.7}Sr_{0.3}Mn_{1-x}Cu_xO_3$ ($x = 0.05$, 0.1) manganites. They showed that, for $\Delta H = 1.35$ T, the ΔS_M reached values of -1.96 and -2.07 J/kg K for $x = 0.05$ and 0.1 compositions, respectively. Later on, Phan et al. [63] significantly improved the MCE of these samples by optimizing the annealing conditions. For $\Delta H = 1$ T, the maximum ΔS_M of the Cu-doped samples was found to be -3.05 J/kg K at 345 K for $x = 0.05$ and ~3.24 J/kg K at 347 K for $x = 0.10$, while it is -2.8 J/kg K at 294 K for Gd metal [3]. These materials are promising for AMR above room temperature. In another work, Phan et al. [54] also found the large magnetic entropy changes in $La_{0.845}Sr_{0.155}Mn_{1-x}M_xO_3$ (M = Cu, Co) Cu-doped manganites. The ΔS_M values are summarized in Table 1. However, the Curie temperatures of these samples were reduced well below room temperature, which is not desirable for room-temperature AMR.

The influence of Ni partial substitution for Mn on the MCE of $La_{0.7}Sr_{0.3}Mn_{1-x}Ni_xO_3$ ($x = 0.01$, 0.02, 0.03, and 0.05) manganites was investigated by Choudhury et al. [64]. It was experimentally observed that for $\Delta H = 1.35$, the ΔS_M values were -2.67, -3.15, -3.54, and -2.33 J/kg K for $x = 0.01$, 0.02, 0.03, and 0.05, respectively. Obviously, the $x = 0.02$ sample exhibited the highest ΔS_M among the compositions investigated. In addition, the large magnetic entropy change of this sample was obtained at 320 K. This indicates that the $x = 0.02$ sample has potential for room-temperature AMR. In a more detailed investigation, Phan et al. [65] revealed that the ΔS_M of the $La_{0.7}Sr_{0.3}Mn_{1-x}Ni_xO_3$ ($x = 0.02$) sample could reach a value as high as -7.65 J/kg K at 350 K for $\Delta H = 7$ T. It is interesting to note that, even under high magnetic fields, the ΔS_M distribution of this material was much more uniform than that of Gd [3] and several polycrystalline perovskite manganites [13], which is desirable for an Ericson-cycle magnetic refrigerator. It is also suggested that such a small amount (~2%) of substitution of Mn^{3+} by a magnetic ion (Ni^{3+}, or Co^{3+}) in the perovskite manganite could favor the spin order and hence the MCE. This investigation opens a window to explore the active MR at high temperatures.

4.2.6. $(La–Nd–Ca)(Mn–M')O_3$ where $M' = Cr$ and Fe

The MCEs of $La_{0.65}Nd_{0.05}Ca_{0.3}Mn_{0.9}M_{0.1}O_3$ (M = Cr, Fe) compounds were investigated by Wang et al. [66]. It was shown that the substitution of Cr or Fe for Mn resulted in a significant decrease in both the MCE and the Curie temperature (see Table 1). In this case, it is suggested that the substitution of Cr or Fe for Mn could greatly weaken the double-exchange ferromagnetic interaction of Mn^{3+}–O–Mn^{4+} and hence reduce the ΔS_M. In general, these materials are not suitable for AMR.

4.2.7. $(Nd_{1-x}M_x)MnO_3$ where $M = Ca$ and Sr

A number of works involving MCEs were conducted on $Nd_{1-x}M_xMnO_3$ (M = Ca or Sr) manganites with charge order, which underwent two successive phase transitions; one is the first-order antiferromagnetic to ferromagnetic transition at lower temperature and the other belongs to the second-order ferromagnetic–metallic-to-paramagnetic–insulator transition at higher temperature [67,68].

Sande et al. [67] first observed the large ΔS_M of 2.8 J/kg K at the charge-ordering temperature of 155 for $\Delta H =$ 1 T in $Nd_{0.5}Sr_{0.5}MnO_3$. They showed that the magnitude of ΔS_M obtained around the first-order transition is about three times larger than that obtained around the second-order one. This is likely related to the suppression of charge ordering, with an increase of accessible states due to the enhancement of electron mobility, under an applied magnetic field. Later on, Chen and Du [68] reported a larger MCE value of $Nd_{0.5}Sr_{0.5}MnO_3$. They showed that the ΔS_M reached a value as high as 7.5 J/kg K at 183 K for $\Delta H = 1$ T. This value of ΔS_M is much larger than that of Gd.

In contrast to the works [67,68], Chau et al. [69] reported a much smaller value of ΔS_M of 1.9 J/kg K at ~155 K for $\Delta H = 1.35$ T in the same composition of $Na_{0.5}Sr_{0.5}MnO_3$. This discrepancy could arise from the different sample preparation (i.e., the annealing temperature and annealing time). In fact, it should be noted that the change in magnetization with respect to temperature occurred much more sharply in the cases [67,68] than in the case [69] and this is the reason leading to a larger variation in the ΔS_M [67,68]. The authors [69] also found a significant decrease in the MCE of $Nd_{0.5}Sr_{0.5}Mn_{1-x}Cu_xO_3$ ($x = 0.02$, 0.1) manganites with Cu substitution for Mn. This could be understood due to the fact that the charge-ordering behavior was drastically modified by Cu doping.

It is generally thought that the charge-order transition temperature of charge-ordered manganites could be modified by doping and this allows making active magnetic refrigerants for magnetic refrigerators [67,68]. It should be noted that, although the charge-ordering manganite has large ΔS_M induced by low magnetic field change, this charge-ordering state is strongly doping- and magnetic field dependent [67–69]. When an applied magnetic field is sufficiently high, the charge-ordered state will be melted and an insulator–metal transition is induced. Indeed, the charge-ordered state was strongly modified, or even

disappeared, under high magnetic fields (~3 T) [22]. It is therefore difficult to apply high fields (~5 T) to achieve the high magnetic cooling efficiency. In addition, even if the charge-order transition temperature of the material is tuned by doping, a sharp charge-ordering magnetic transition will be modified thereby leading to a considerable reduction in the MCE [69]. Another disadvantage is that the FWHM of MCE peak is only several K, followed by large thermal and field hysteresis, which is not beneficial for AMR.

4.2.8. $(Pr_{1-x}M_x)MnO_3$ where M = Ca, Sr and Pb

Gomes et al. [70] investigated the MCEs of $Pr_{1-x}Ca_xMnO_3$ ($0.3 \leqslant x \leqslant 0.45$) manganites, who showed the large positive and negative changes of ΔS_M. It was experimentally observed that $Pr_{0.68}Ca_{0.32}MnO_3$ exhibited, respectively, the positive and negative ΔS_M of 24 J/kg K at 21.5 K and −27 J/kg K at 31 K for $\Delta H = 5$ T. This material could be good for MR at low temperatures. In addition, these authors [71,72] studied the charge-ordering contribution to the magnetic entropy change of $Pr_{1-x}Ca_xMnO_3$ ($0.2 \leqslant x \leqslant 0.95$) manganites. They suggested that the ΔS_M of $Pr_{1-x}M_xMnO_3$ ($0.3 < x < 0.90$) charge-ordered manganites around the charge-ordering temperature was related to a negative contribution from the spin ordering ΔS_{spin}, which was superimposed to a positive contribution due to the charge-ordering ΔS_{CO}.

In another work, the MCEs of $Pr_{1-x}Sr_xMnO_3$ ($x = 0.3$, 0.4, and 0.5) polycrystalline manganites were investigated by Chen et al. [73], who found the largest ΔS_M of 7.1 J/kg K at 160 K for $\Delta H = 1$ T for the $x = 0.5$ sample. This value of ΔS_M is much larger than that of Gd, $\Delta S_M = -2.8$ J/kg K for $\Delta H = 1$ T. This material could be good for MR in the corresponding temperature range. More interestingly, Phan et al. [74] found a large MCE in a single crystal of $Pr_{0.63}Sr_{0.37}MnO_3$, which underwent a very sharp ferromagnetic-to-paramagnetic phase transition at ~300 K. The ΔS_M of −8.52 J/kg K and the ΔT_{ad} of 5.65 K for $\Delta H = 5$ T were found to occur around 300 K, thereby allowing water to be used as a heat transfer fluid in the room-temperature MR regime. In addition, the ΔS_M distribution is very uniform and therefore desirable for an Ericson-cycle magnetic refrigerator. The large magnetic entropy change induced by a relatively low magnetic field change is beneficial for household application of active magnetic refrigerant materials. These make the $Pr_{0.63}Sr_{0.37}MnO_3$ single crystal a competitive candidate for commercial applications of room-temperature MR.

Recently, the new finding of large low-field MCEs in polycrystalline $Pr_{1-x}Pb_xMnO_3$ ($0.1 \leqslant x \leqslant 0.5$) manganites was reported by Phan et al. [75]. It was shown that, for $\Delta H = 1.35$ T, the ΔS_M reached values of −3.91, −3.68 and −3.34 J/kg K for $x = 0.1$, 0.4 and 0.5 compositions, respectively. These values are larger than that of Gd (−3.32 J/kg K) and were attained by a low applied magnetic field that can be generated by permanent magnets. These superior magnetocaloric features together with a relatively low material cost make $Pr_{1-x}Pb_xMnO_3$ attractive candidate materials for MR in the temperature range of 150–270 K.

4.2.9. $(La_{1-x}M_x)_3Mn_2O_7$ where M = Ca and K

The giant MCEs were discovered in the new two-layered manganites of $La_{1.6}Ca_{1.4}Mn_2O_7$ [76] and $La_{1.4}Ca_{1.6}Mn_2O_7$ [77]. Zhou et al. [76] showed that, for $\Delta H = 1.5$ T, the ΔS_M of $La_{1.6}Ca_{1.4}Mn_2O_7$ reached a maximum of −3.8 J/kg K at 168 K. More interestingly, Zhu et al. [77] found a large ΔS_M of −17 J/kg K at 270 K for $\Delta H = 5$ T in the $La_{1.4}Ca_{1.6}Mn_2O_7$ compound. This value of ΔS_M is much larger than that of Gd (~10.2 J/kg K) [3] and is close to that of $Gd_5Si_2Ge_2$ [11] or $MnFeP_{0.45}As_{0.55}$ (~18 J/kg K) [16] for $\Delta H = 5$ T. Another advantage is that the two-layered manganites have a broad FWHM of the MCE peak, resulting in the high cooling capacity. Indeed, the refrigerant capacity of $La_{1.4}Ca_{1.6}Mn_2O_7$ is larger than that of Gd [77]. This material could be ideal for sub-room-temperature MR.

Zhong et al. [78] investigated the MCEs of $La_{2.5-x}K_{0.5+x}Mn_2O_7$ ($x = 0.05$, 0.15, 0.25, 0.35, and 0.45) two-layered manganites and found an increase in both ΔS_M and T_C with increasing K-doped content up to $x = 0.35$. For $\Delta H = 1$ T, the largest ΔS_M was obtained to be −2 J/kg K at 250 K for $x = 0.35$ composition. In general, these materials could be used as magnetic refrigerants for MR in the intermediate temperature range of 150–270 K.

4.2.10. Advantage of single crystalline manganites

Most magnetocaloric manganites investigated are polycrystalline materials, which actually show some certain disadvantages. For instance, such a non-uniform MCE curve (e.g., the ΔS_M vs. T curve) distribution—which is not desirable for an Ericsson-cycle magnetic refrigerator—has often been observed in *polycrystalline* manganites, due to structural inhomogeneity [13,50–60].

In this context, Phan et al. [11,51,74,79–81] discovered that *single crystalline* manganites have superior magnetocaloric properties to *polycrystalline* manganites. It has been shown that the ΔS_M value is larger in the single-crystalline manganite than that in the polycrystalline one as shown in Fig. 3 [80]. More interestingly, the adiabatic temperature change (ΔT_{ad}) is larger in the single-crystalline manganite than that in the polycrystalline one (see Fig. 4). In addition, the single crystals have the large magnetic entropy change induced by low magnetic field change (<2 T), which is beneficial for the household application of AMR materials [11,51,74]. This has also been verified by Terashita et al. [16], who showed that the change of the heat capacity with respect to an applied magnetic field occurred more strongly for the single crystalline manganite than for the polycrystalline one. More interestingly, the symmetrical and uniform distribution of $\Delta S_M(T)$ can be seen only for the single crystal (see Fig. 3(a)), even under high magnetic

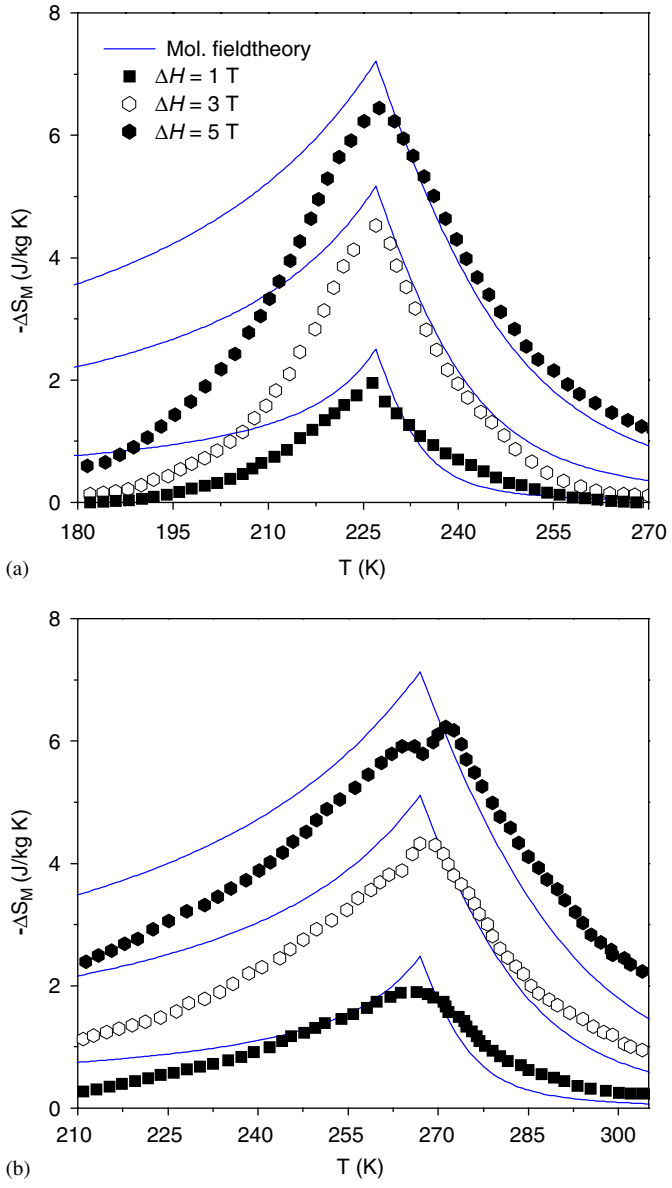

Fig. 3. The magnetic entropy change, ΔS_M, as a function of temperature in various fields for $La_{0.7}Ca_{0.3}MnO_3$: (a) single crystal, (b) polycrystalline. The solid line indicates for the molecular field calculations.

fields [11,80]. This is ascribed to the absence of grains in such a single-crystalline material.

In contrast to this, considerable and asymmetrical variations of the $\Delta S_M(T)$ curves with external magnetic field, especially under high fields, in the polycrystalline manganite (see Fig. 3(b)) were observed and are likely due to the grain boundary effects [13]. The non-uniform distribution of $\Delta S_M(T)$ in polycrystalline manganites is also believed to be ascribed to a spread of the ferromagnetic transition temperature in different ferromagnetic clusters caused by the inhomogeneity of structure and stoichiometry [61]. This feature negatively affects the magnetic cooling efficiency of a magnetic refrigerator. Besides, single crystalline manganites have been found to show much smaller thermal and field hysteresis compared

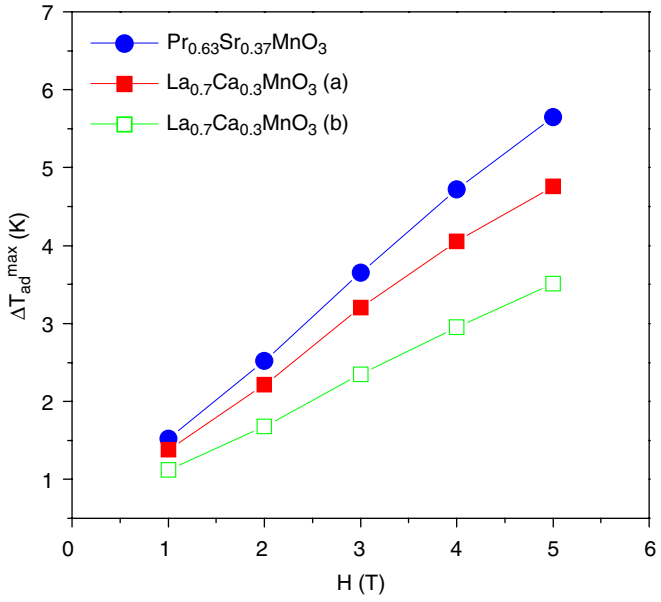

Fig. 4. The maximum adiabatic temperature change, ΔT_{ad}, is plotted against applied magnetic field for a $Pr_{0.63}Sr_{0.37}MnO_3$ single crystal and $La_{0.7}Ca_{0.3}MnO_3$: (a) single crystal, (b) polycrystalline.

to polycrystalline ones [82]. These results indicate that the single-crystalline manganites are excellent candidates as working materials for AMR [11,74].

4.2.11. Theoretical evaluation of MCE

The molecular field model has often been used to describe qualitatively the magnetic entropy change (ΔS_M) and the adiabatic temperature change (ΔT_{ad}) of a magnetocaloric manganite [12,20,80]. It has been shown that the theoretical calculations using the molecular field model provide a fairly good description of the magnetic entropy change above T_C, but the magnetic entropy change is overestimated below T_C. As an example displayed in Fig. 3 for the $La_{0.7}Ca_{0.3}MnO_3$ sample, the discrepancy between the theoretical calculations and the experimental data can be attributed to roughness of the model. It should be noted that this model did not take into account the roles played by the charge ordering and the Jahn–Teller effect, which actually affect the MCE value even for the case of conventional ferromagnetic manganites [12,20]. This thus warrants further study. Nevertheless, the molecular field model has been useful for describing qualitatively the magnetic entropy change and the adiabatic temperature change, particularly at temperatures close to the Curie temperature.

4.3. Comparison of magnetocaloric materials

It is obvious from Table 1 that each manganite material system can be useful for MR at various temperatures. As far as the room-temperature AMR is concerned, our attention has been paid to magnetocaloric materials which show large low-field MCEs in the room-temperature range. To this event, we display in Fig. 5 the MCEs of several

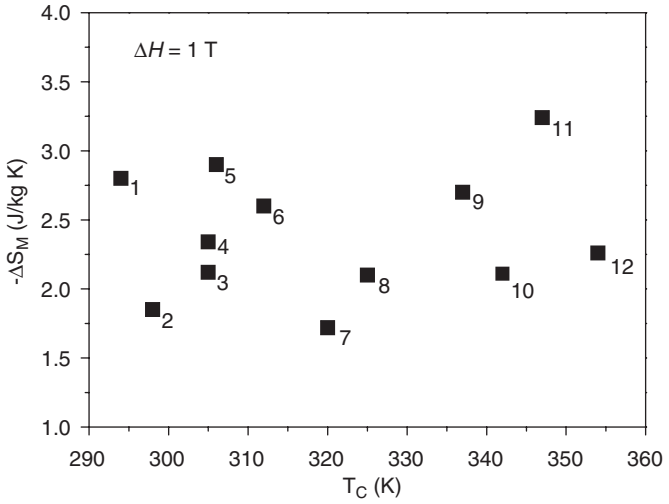

Fig. 5. The magnetic entropy change, ΔS_M, for $\Delta H = 1$ T for the potential magnetocaloric manganites for room-temperature magnetic refrigeration. Symbols: 1—Gd; 2—$La_{0.7}Ca_{0.18}Ba_{0.12}MnO_3$ [42]; 3—$La_{0.65}Sr_{0.35}MnO_3$ [13]; 4—$La_{0.7}Ca_{0.2}Sr_{0.1}MnO_3$ [11]; 5—$La_{0.78}Ag_{0.22}MnO_3$ [27]; 6—$La_{2/3}Ba_{1/3}MnO_{2.98}$ [43]; 7—$La_{0.7}Ca_{0.18}Ba_{0.12}MnO_3$ [42]; 8—$La_{0.75}Ca_{0.1}Sr_{0.15}MnO_3$ [47]; 9—$La_{2/3}Ba_{1/3}MnO_3$ [43]; 10—$La_{0.835}Na_{0.165}MnO_3$ [23]; 11—$La_{0.7}Sr_{0.3}Mn_{0.90}Cu_{0.10}O_3$ [63]; 12—$La_{0.6}Sr_{0.2}Ba_{0.2}MnO_3$ [13].

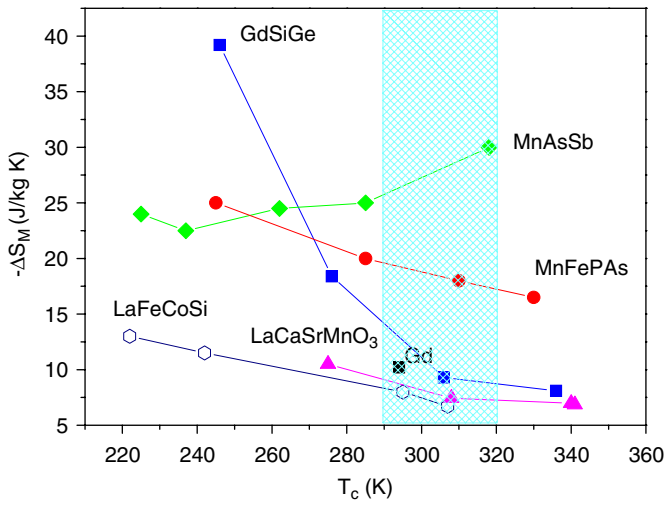

Fig. 6. The magnetic entropy change, ΔS_M, is plotted against the Curie temperature (T_C) for $\Delta H = 5$ T for the potential magnetocaloric candidate materials for magnetic refrigeration in the sub-room and room-temperature range. The material compositions are $MnAs_{1-x}Sb_x$ ($x = 0$, 0.1, 0.15, 0.25, 0.3) [8], $La(Fe_{1-x}Co_x)_{11.2}Si_{1.8}$ ($x = 0$, 0.02, 0.07, 0.08) [9], and $La_{0.7}Ca_{0.3-x}Sr_xMnO_3$ ($x = 0.05$, 0.10, 0.15, 0.25) [11], $Gd_5(Si_xGe_{1-x})_4$ ($x = 0.43$, 0.50, 0.515, 1) [18], $MnFeP_{1-x}As_x$ ($x = 0.45$, 0.50, 0.55, 0.65) [84].

magnetic refrigerant candidate manganites in comparison with Gd for a small magnetic field change of 1 T. It is interesting to see that the magnitude of MCE of several manganites is comparable to that of Gd and, more interestingly, the MCE peak temperature can be easily tuned in the temperature range of 290–360 K by selecting suitable manganites (see Fig. 5). This indicates that these manganites are potential for room-temperature AMR.

In order to compare with other magnetocaloric materials, we display in Figs. 6 and 7 the dependences of the magnetic entropy change (ΔS_M) and the relative cooling power RCP(S) on the Curie temperature. From the figures, it can be stated that the $Gd_5(Si_xGe_{1-x})_4$ ($0 \leqslant x \leqslant 1$) alloys are the most promising for sub-room-temperature AMR, because the largest MCEs have been achieved in the temperature range of 250–290 K [3]. Although the variation of the Si/Ge ratio allows the tuning of the MCE peak temperature in the wide temperature range of 20–330 K, the MCE values are obviously dropped strongly in the room-temperature range (see Fig. 6). In the temperature range of 290–320 K which is applicable for room-temperature AMR, the $MnAs_{1-x}Sb_x$ ($0 \leqslant x \leqslant 0.4$) materials show the largest value of MCE (see Fig. 6) but do relatively small RCP(S) (see Fig. 7). In addition, these materials possess serious problems of large thermal and field hysteresis, which are not beneficial for AMR. This might be an additional challenge for magnetic refrigerant materials showing GMC effects due to the first-order structural/magnetic transition. It can be stated from Figs. 6 and 7 that the $MnFeP_{1-x}As_x$ ($0.25 \leqslant x \leqslant 0.65$) materials with reversible/large MCEs and the relatively high magnetic-ordering temperatures are the most promising candidates for room-temperature AMR applications [4]. The variation of the

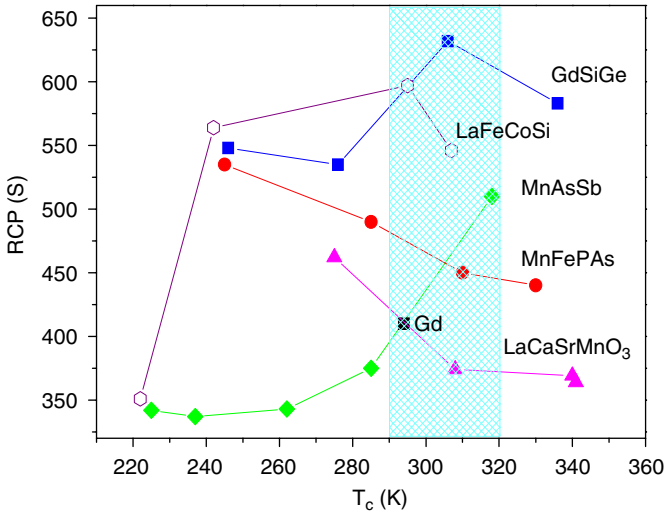

Fig. 7. The relative cooling power RCP(S) is plotted against the Curie temperature (T_C) for $\Delta H = 5$ T for the potential magnetocaloric candidate materials for magnetic refrigeration in the sub-room and room-temperature range. The material compositions are $MnAs_{1-x}Sb_x$ ($x = 0$, 0.1, 0.15, 0.25, 0.3) [8], $La(Fe_{1-x}Co_x)_{11.2}Si_{1.8}$ ($x = 0$, 0.02, 0.07, 0.08) [9], and $La_{0.7}Ca_{0.3-x}Sr_xMnO_3$ ($x = 0.05$, 0.10, 0.15, 0.25) [11], $Gd_5(Si_xGe_{1-x})_4$ ($x = 0.43$, 0.50, 0.515, 1) [18], $MnFeP_{1-x}As_x$ ($x = 0.45$, 0.50, 0.55, 0.65) [84].

P/S ratio between 3/2 and $\frac{1}{2}$ makes it possible to tune the optimal operating temperature between 200 and 350 K, while retaining relatively large MCE values. The problems of thermal and field hysteresis are less concerned in $MnFeP_{1-x}As_x$ than in $Gd_5(Si_xGe_{1-x})_4$ and $MnAs_{1-x}Sb_x$, but the releasing of As and/or P into our living environment is of serious concern of the $MnFeP_{1-x}As_x$ materials

and this may lead to extra costs in the manufacturing process. Nonetheless, from a commercial point of view, it is believed that the magnetic materials composed of 3d-transition metals are more adequate than the rare earths. Several magnetocaloric materials have been found to show larger MCE and RCP(S), but if taking all the requirements for a magnetocaloric material (Section 2.5) into account then Gd is still the best magnetic refrigerant for room-temperature AMR [3,4]. That is why such Gd materials have been mainly used in currently room-temperature magnetic refrigerators, even though the materials cost is very expensive [4].

Manganite magnetocaloric materials can be promising candidates for AMR, because they show the large MCEs that are comparable to Gd and other magnetic refrigerant candidate materials. One disadvantage of this typical material is that the adiabatic temperature change is not very large due to the relatively high heat capacity [80,83]. This may be somewhat limiting such manganites for AMR technology. However, this task will be overcome because of the rapid development of the magnetic cooling technology as of today. It is interesting to note that, when compared with Gd and other candidate materials, such perovskite manganites are more convenient to prepare and exhibit higher chemical stability as well as higher resistivity that is favorable for lowering eddy current heating. In addition, the manganites possess much smaller thermal and field hysteresis than any rare earth and 3d-transition metal-based alloys. The MCE peak temperature can be easily tuned in the wide temperature range of 100–375 K, which is beneficial for AMR at various temperatures. In addition, the manganite materials are cheapest (~$10/kg) among the existing magnetic refrigerants [4]. These superior features make them more promising for future MR technology.

5. Concluding remarks

Progress in magnetic refrigeration technology, especially in room-temperature magnetic refrigeration, has been recognized worldwide. This enabling technology will firmly replace the CGC technology in the near future. The discoveries of outstanding magnetocaloric materials have provided new opportunities to use them as alternative working materials in active magnetic refrigerators at various temperatures. It is believed that the manganite materials with the superior magnetocaloric properties in addition to cheap materials processing cost will be the option of future magnetic refrigeration technology.

Acknowledgments

This article is dedicated to Prof. Nguyen Chau on his healthy recovery. The authors wish to acknowledge our long-standing collaborators: Prof. Nguyen Chau and Mr. Nguyen Duc Tho at Hanoi University of Science (Viet Nam), Prof. Nam Hwi Hur at Korea Research Institute of Standards and Science (South Korea), Dr. A.N. Ulyanov at Donetsk Physico-Technical Institute of National Academy of Sciences (Ukraine), Dr. Hua-Xin Peng at University of Bristol (England). Special thanks are also due to all members of the Applied Physics Laboratory, Chungbuk National University, South Korea, for their experimental assistance. Research at the Chungbuk National University was supported by the Korean Science and Engineering Foundation through the Research Center for Advance Magnetic Materials at Chungnam National University.

References

[1] A.M. Tishin, in: K.H. Buschow (Ed.), Handbook of Magnetic Materials, vol. 12, North-Holland, Amsterdam, 1999, pp. 395–524.
[2] E. Warburg, Ann. Phys. 13 (1881) 141.
[3] V.K. Pecharsky, K.A. Gschneidner, A.O. Tsokol, Rep. Prog. Phys. 68 (2005) 1479.
[4] E. Bruck, J. Phys. D: Appl. Phys. 38 (2005) R381.
[5] W.F. Giauque, D.P. MacDougall, Phys. Rev. 43 (1933) 768.
[6] V.K. Pecharsky, K.A. Gschneidner, Phys. Rev. Lett. 78 (1997) 4494.
[7] F.X. Hu, B.G. Shen, J.R. Sun, G.H. Wu, Phys. Rev. B 64 (2001) 132412.
[8] H. Wada, Y. Tanabe, Appl. Phys. Lett. 79 (2001) 3302.
[9] S. Fujieda, A. Fujita, K. Fukamichi, Appl. Phys. Lett. 81 (2002) 1276.
[10] Q. Tegus, E. Bruck, K.H. Buschow, F.R. de Boer, Nature 415 (2002) 150.
[11] M.H. Phan, S.C. Yu, N.H. Hur, Appl. Phys. Lett. 86 (2005) 072504.
[12] A. Szewczyk, H. Szymczak, A. Wisniewski, K. Piotrowski, R. Kartaszynski, B. Dabrowski, S. Kolesnik, Z. Bukowski, Appl. Phys. Lett. 77 (2000) 1026.
[13] M.H. Phan, S.B. Tian, D.Q. Hoang, S.C. Yu, C. Nguyen, A.N. Ulyanov, J. Magn. Magn. Mater. 258–259 (2003) 309.
[14] Y. Sun, M.B. Salamon, S.H. Chun, J. Appl. Phys. 92 (2002) 3235.
[15] S.W. Biernacki, H.J. Schulz, Phys. Rev. B 70 (2004) 092405.
[16] H. Terashita, B. Myer, J.J. Neumeier, Phys. Rev. B 72 (2005) 132415.
[17] C.M. Xiong, J.R. Sun, Y.F. Chen, B.G. Shen, J. Du, Y.X. Li, IEEE Trans. Magn. 41 (2005) 122.
[18] V.K. Pecharsky, K.A. Gschneidner, Annu. Rev. Mater. Sci. 30 (2000) 387.
[19] V.K. Pecharsky, K.A. Gschneidner, A.O. Percharsky, A.M. Tishin, Phys. Rev. B 64 (2001) 144406.
[20] A. Szewczyk, M. Gutowska, K. Piotrowski, B. Dabrowsk, J. Appl. Phys. 94 (2003) 1873.
[21] A. Szewczyk, M. Gutowska, B. Dabrowski, T. Plackowski, N.P. Danilova, Y.P. Gaidukov, Phys. Rev. B 71 (2005) 224432.
[22] Y. Tokura (Ed.), Colossal Magnetoresistive Oxides (Advances in Condensed Materials Science), vol. 2, Gordon and Breach Science Publishers, Amsterdam, 2000.
[23] W. Zhong, W. Cheng, W.P. Ding, N. Zhang, Y.W. Du, Q.J. Yan, Solid State Commun. 106 (1998) 55.
[24] W. Zhong, W. Cheng, W.P. Ding, N. Zhang, A. Hu, Eur. Phys. J. B 3 (1998) 169.
[25] W. Zhong, W. Cheng, W.P. Ding, N. Zhang, A. Hu, J. Magn. Magn. Mater. 195 (1999) 112.
[26] T. Tang, K.M. Gu, Q.Q. Cao, D.H. Wang, S.Y. Wang, S.Y. Zhang, Y.W. Du, J. Magn. Magn. Mater. 222 (2000) 110.
[27] N.T. Hien, N.P. Thuy, Physica B 319 (2002) 168.
[28] D.T. Morelli, A.M. Mance, J.V. Mantese, A.L. Micheli, J. Appl. Phys. 79 (1996) 373.
[29] Z.B. Guo, Y.W. Du, J.S. Zhu, H. Huang, W.P. Ding, D. Feng, Phys. Rev. Lett. 78 (1997) 1142.
[30] Z.B. Guo, J.R. Zhang, H. Huang, W.P. Ding, Y.W. Du, Appl. Phys. Lett. 70 (1996) 904.

[31] X.X. Zhang, J. Tejada, Y. Xin, G.F. Sun, K.W. Wong, X. Bohigas, Appl. Phys. Lett. 69 (1996) 3596.
[32] Y. Sun, X. Xu, Y.H. Zhang, J. Magn. Magn. Mater. 219 (2000) 183.
[33] J. Mira, J. Rivas, L.E. Hueso, F. Rivadulla, M.A. Lopez Quintela, J. Appl. Phys. 91 (2002) 8903.
[34] G.C. Lin, Q. Wei, J.X. Zhang, J. Magn. Magn. Mater. 300 (2006) 392.
[35] Q.Y. Xu, K.M. Gu, X.L. Liang, G. Ni, Z.M. Wang, H. Sang, Y.W. Du, J. Appl. Phys. 90 (2001) 524.
[36] L.E. Hueso, P. Sande, D.R. Miguens, J. Rivas, F. Rivadulla, M.A. Lopez-Quintela, J. Appl. Phys. 91 (2002) 9943.
[37] M.H. Phan, S.C. Yu, N.H. Hur, J. Magn. Magn. Mater. 262 (2003) 407.
[38] M.H. Phan, S.C. Yu, Y.M. Moon, N.H. Hur, J. Magn. Magn. Mater. 272–276 (2004) e503.
[39] D.L. Hou, Y. Bai, J. Xu, G.D. Tang, X.F. Nie, J. Alloys Compd. 384 (2004) 62.
[40] R.V. Demin, L.I. Koroleva, Phys. Solid State 46 (2004) 1081.
[41] Y. Xu., U. Memmert, U. Hartmann, J. Magn. Magn. Mater. 242–245 (2002) 698.
[42] M.H. Phan, S.B. Tian, S.C. Yu, A.N. Ulyanov, J. Magn. Magn. Mater. 256 (2003) 306.
[43] W. Zhong, W. Cheng, C.T. Au, Y.W. Du, J. Magn. Magn. Mater. 261 (2003) 238.
[44] N.H. Luong, D.T. Hanh, N. Chau, N.D. Tho, T.D. Hiep, J. Magn. Magn. Mater. 290–291 (2005) 690.
[45] N. Chau, H.N. Nhat, N.H. Luong, D.L. Minh, N.D. Tho, N.N. Chau, Physica B 327 (2003) 270.
[46] S.G. Min, K.S. Kim, S.C. Yu, H.S. Suh, S.W. Lee, IEEE Trans. Magn. 41 (2005) 2760.
[47] Z.B. Guo, W. Yang, Y.T. Shen, Y.W. Du, Solid State Commun. 105 (1998) 89.
[48] M.H. Phan, S.C. Yu, A.N. Ulyanov, H.K. Lachowicz, Mater. Sci. 21 (2003) 133.
[49] G.C. Lin, C.D. Xu, J.X. Zhang, J. Magn. Magn. Mater. 283 (2004) 375.
[50] G.C. Lin, C.D. Xu, Q. Wei, J.X. Zhang, Mater. Lett. 59 (2005) 2149.
[51] M.H. Phan, S.C. Yu, N.H. Hur, J. Magn. Magn. Mater. 290–291 (2005) 665.
[52] W. Chen, L.Y. Nie, W. Zhong, Y.J. Shi, J.J. Hu, A.J. Li, Y.W. Du, J. Alloys Compd. 395 (2005) 23.
[53] M.H. Phan, S.C. Yu, N. Chau, J. Magn. Magn. Mater., unpublished.
[54] M.H. Phan, T.L. Phan, S.C. Yu, N.D. Tho, N. Chau, Phys. Stat. Sol. (b) 241 (2004) 1744.
[55] Z.M. Wang, G. Ni, Q.Y. Xu, H. Sang, Y.W. Du, J. Appl. Phys. 90 (2001) 5689.
[56] H. Gencer, S. Atalay, H.I. Adiguzel, V.S. Kolat, Physica B 357 (2005) 326.
[57] H. Chen, C. Lin, D.S. Dai, J. Magn. Magn. Mater. 257 (2003) 254.
[58] G. Wang, Z.D. Wang, L.D. Zhang, Mater. Sci. Eng. B 116 (2005) 183.
[59] X. Bohigas, J. Tejada, E. Del Barco, X.X. Zhang, M. Sales, Appl. Phys. Lett. 73 (1998) 390.
[60] J.A. Barclay, J. Alloys Compd. 207–208 (1994) 355.
[61] Y. Sun, W. Tong, Y.H. Zhang, J. Magn. Magn. Mater. 232 (2001) 205.
[62] N. Chau, P.Q. Niem, H.N. Nhat, N.H. Luong, N.D. Tho, Physica B 327 (2003) 214.
[63] M.H. Phan, H.X. Peng, S.C. Yu, N. Tho, N. Chau, J. Magn. Magn. Mater. 285 (2005) 199.
[64] M.A. Choudhury, S. Akhter, D.L. Minh, N.D. Tho, N. Chau, J. Magn. Magn. Mater. 272–276 (2004) 1295.
[65] M.H. Phan, N.D. Tho, N. Chau, S.C. Yu, M. Kurisu, J. Appl. Phys 97 (2005) 3215.
[66] Z.M. Wang, G. Ni, Q.Y. Xu, H. Sang, Y.W. Du, J. Magn. Magn. Mater. 234 (2001) 371.
[67] P. Sande, L.E. Hueso, D.R. Miguens, J. Rivas, F. Rivadulla, M.A. Lopez-Quintela, Appl. Phys. Lett. 79 (2001) 2040.
[68] P. Chen, Y.W. Du, Chin. J. Phys. 39 (2001) 357.
[69] N. Chau, D.H. Cuong, N.D. Tho, H.N. Nhat, N.H. Luong, B.T. Cong, J. Magn. Magn. Mater. 272–276 (2004) 1292.
[70] A.M. Gomes, F. Garcia, A.P. Guimaraes, M.S. Reis, V.S. Amaral, P.B. Tavares, J. Magn. Magn. Mater. 290–291 (2005) 694.
[71] M.S. Reis, A.M. Gomes, J.P. Araujo, J.S. Amaral, P.B. Tavares, I.S. Oliveira, V.S. Amaral, J. Magn. Magn. Mater. 290–291 (2005) 697.
[72] M.S. Reis, A.M. Gomes, J.P. Araujo, P.B. Tavares, I.S. Oliveira, V.S. Amaral, J. Magn. Magn. Mater. 290–291 (2005) 697.
[73] P. Chen, Y.W. Du, G. Ni, Europhys. Lett. 52 (2000) 589.
[74] M.H. Phan, H.X. Peng, S.C. Yu, J. Appl. Phys. 97 (2005) 10M306.
[75] M.H. Phan, H.X. Peng, S.C. Yu, D.T. Hanh, N.D. Tho, N. Chau, J. Appl. Phys. 99 (2006) 08Q108.
[76] T.J. Zhou, Z. Yu, W. Zhong, X.N. Xu, H.H. Zhang, Y.W. Du, J. Appl. Phys. 85 (1999) 7975.
[77] H. Zhu, H. Song, Y.H. Zhang, Appl. Phys. Lett. 81 (2002) 3416.
[78] W. Zhong, W. Chen, H.Y. Jiang, X.S. Liu, C.T. Au, Y.W. Du, Eur. Phys. J. B 30 (2002) 331.
[79] M.H. Phan, S.B. Tian, S.C. Yu, N.H. Hur, Physica B 327 (2003) 211.
[80] M.H. Phan, S.C. Yu, N.H. Hur, Y.H. Yeong, J. Appl. Phys. 96 (2004) 1154.
[81] M.H. Phan, V.T. Pham, S.C. Yu, J.R. Rhee, N.H. Hur, J. Magn. Magn. Mater 272–276 (2004) 2337.
[82] M.H. Phan, Phys. Rev. Lett., unpublished.
[83] X. Bohigas, J. Tejada, M.L. Marinez-Sarrion, S. Tripp, R. Black, J. Magn. Magn. Mater. 208 (2000) 85.
[84] Q. Tegus, E. Bruck, L. Zhang, W. Dagula, K.H.J. Buschow, F.R. de Boer, Physica B 319 (2002) 174.